SWIFT XRT CALDB RELEASE NOTE

SWIFT-XRT-CALDB-09:

Epoch Dependent $V_{ss} = 6\,V$ Response Matrices

Table P1: Files released on 2024-Apr-30:

Filename	Mode	Grade	Substrate[†] voltage (V)	Start Date	End Date
swxpc0to12s6_20210101v016.rmf swxpc0to4s6_20210101v016.rmf swxpc0s6_20210101v016.rmf	PC	$0-12$ $0-4$ 0	6	2021-Jan-01	—
swxwt0to2s6_20210101v017.rmf swxwt0s6_20210101v017.rmf	WT	$0-2$ 0	6	2021-Jan-01	—

[†] The substrate voltage was permanently raised from $V_{ss} = 0\,V$ to $V_{ss} = 6\,V$ on 2007-Aug-30 (see below).

Scope of Document

This document describes the release of further epoch dependent *Swift*-XRT Photon Counting (PC) mode and Windowed Timing (WT) redistribution matrix files (RMFs), appropriate for substrate voltage 6V (i.e. $V_{ss} = 6\,\text{V}$) data taken after 2021-Jan-01, which better match the evolution of the CCD trap-corrected spectral resolution at this time.

Important: The broadened RMFs announced here were originally made available through the HEASARC CALDB on 2024-Mar-27 as file versions v015 for PC mode and v016 for WT mode. However, an error in the first row values of the ENERG_LO *and* E_MIN *columns meant the files were found to be incompatible with the* FTOOLS ftaddrmf *and* ftaddarf *when attempting to combine outputs created from earlier epoch RMFs. The column values have now been corrected and the file version numbers increased accordingly, to* v016 *for PC and* v017 *for WT. The changes do not effect spectral fitting results.*

Introduction

The XRT effective area is made up of three main components: the mirror effective area, the filter transmission and the CCD quantum efficiency (QE). The QE is included directly in the redistribution matrix files (RMFs) while the ancillary response files (ARFs) contain the mirror effective area and the filter transmission.

The XRT RMFs are generated via a Monte-Carlo code, which simulates the interaction of X-rays in the detector as accurately as possible using known physical processes, such as charge-cloud spreading through the active layers of the device and charge transfer inefficiency (CTI) losses when the CCD is read out. As well as accounting for the CCD QE, the RMFs model the response of the detector to incident X-rays and are mode, grade and epoch dependent.

Observation-specific ARF files are produced by the XRTMKARF task (part of the XRTDAS-HEADAS software). This task corrects the nominal (on-axis, infinite extraction region) ARF file from the CALDB for the effects of telescope vignetting and, optionally (*psfflag=yes*), for PSF losses incurred when finite sized extraction regions are used in point source analysis. Additional corrections for CCD defects (caused by 'bad columns' or 'hot-pixels') can be made with the inclusion of an exposure map (with the option *expofile=filename.img*), which can automatically be generated by the data analysis pipeline. The task can also generate ARFs for extended sources (option *extended=yes*), such as clusters of galaxies or supernova remnants.

Motivation behind this release

Over time, the accumulated radiation dose and high-energy proton interactions cause damage to the CCD (in the imaging area, the store frame area and the serial register) resulting in a build-up of charge traps (i.e. faults in the Si crystalline structure of the CCD which hold onto some of the charge released during an X-ray interaction). The deepest traps are responsible for the strongest spectral degradation, causing a monochromatic line to show a more pronounced low energy wing. The most serious of these charge traps can cause a loss of up to $\sim 600\,\text{eV}$ at $6\,\text{keV}$ and $\sim 300\,\text{eV}$ at $1.856\,\text{keV}$ from the incident X-ray energy, although typical values are very much smaller.

For observations taken after 2007-Sep-01, we started mapping the location and depths of the deepest traps found in the CCD and updated the *Swift*-XRT XRTCALCPI software task to provide a trap-corrected energy scale reconstruction to mitigate their effects The gain files are updated annually — see the latest gain file release note SWIFT-XRT-CALDB-04_v24 for details and caveats.

While the application of such trap corrections help restore the spectral resolution (i.e. intrinsic line Full Width at Half Maximum [FWHM]) of the detector, further degradation of the response resolution is to be expected as the number of trapping sites continue to increase with time, causing a distribution of shallower traps not accounted for by the applied trap corrections. Recent observations of line rich sources such as Tycho, Cas A, and SNR 1E0102.2–7219 indicate that further epoch dependent RMF response broadening is required beyond that provided by the $V_{ss} = 6\,\text{V}$ RMFs released on 2014-Jun-10 (described in SWIFT-XRT-CALDB-09_v19).
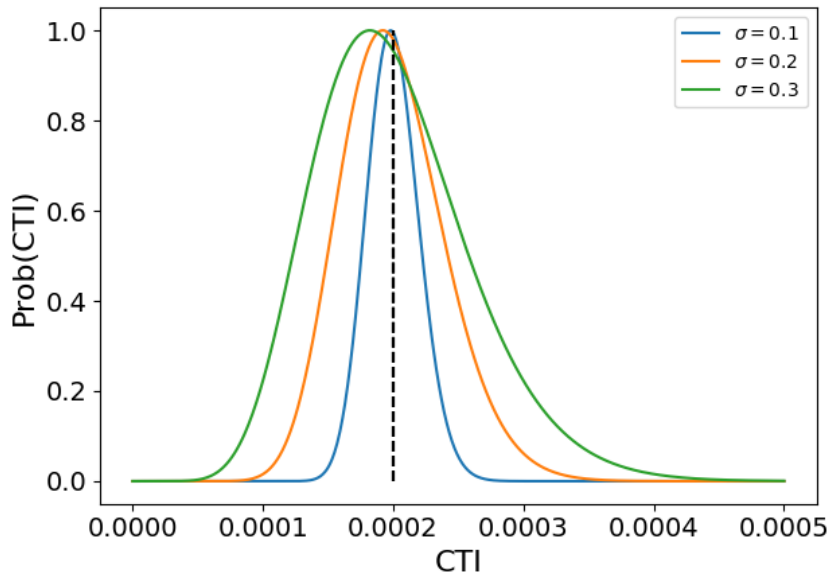
Figure 1: Example CTI distributions, modelled as a Gamma distribution, as a function of the distribution's standard deviation, σ, illustrating its asymmetric nature as σ increases. The dashed vertical line marks the location of the mean CTI value.

Post 2021 Epoch $V_{ss} = 6\,V$ RMFs

Given the findings above, we have started to compute updated epoch-dependent $V_{ss} = 6\,V$ PC and WT RMFs to account for the increase in spectral broadening, starting with data taken since 2021. The RMFs are created assuming an input source of photons which uniformly illuminates the CCD. The 2021 epoch RMFs released here are listed in table P1.

In order to achieve this, as well as increasing the electronic noise and CTI values input to the CCD Monte-Carlo simulator to values appropriate for 2021 data (see table 1), as described in previous release notes (such as SWIFT-XRT-CALDB-09_v19), we have modified the CCD simulator to introduce a level of CTI stochasticity by drawing randomised CTI values from a Gamma distribution (see figure 1). The Gamma distribution has the nice property that it is always positive, like CTI, and becomes asymmetric as its fractional standard deviation (σ_f) increases, with an extended tail, as expected for the distribution of CTI values (Pagani, 2018, priv. comm.). For the 2021 epoch described here, we found σ_f values of 0.2 gave a good match to the line rich SNR calibration spectra.

Table 1: Epoch dependent electronic noise (EN) and CTI values. The former is estimated from PC mode raw frame data while the latter is derived from PC mode Fe-55 corner source data.

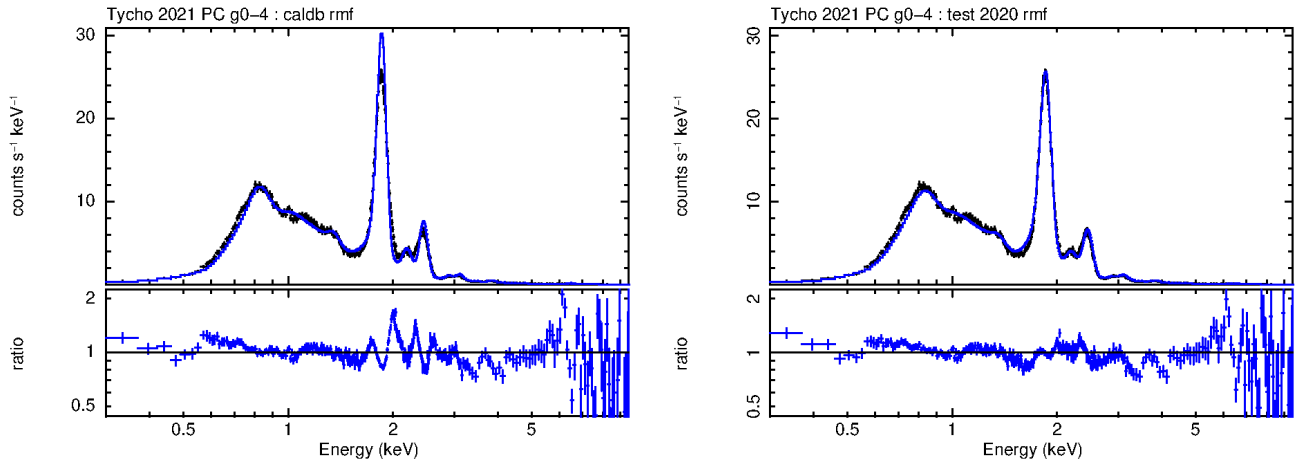| Date	MET (s)	EN (e-)	CTI_s	CTI_p
2009-01-01	2.52e8	7.9	0.34e-4	0.67e-4
2011-01-01	3.16e8	8.8	0.50e-4	1.05e-4
2013-01-01	3.79e8	9.4	0.55e-4	1.50e-4
2014-01-01	4.10e8	9.5	0.70e-4	1.55e-4
2015-01-01	4.42e8	9.8	0.75e-4	1.60e-4
2016-01-01	4.73e8	10.0	0.80e-4	1.65e-4
2017-01-01	5.05e8	10.1	0.82e-4	1.70e-4
2018-01-01	5.36e8	10.3	0.85e-4	1.75e-4
2019-01-01	5.68e8	10.6	0.87e-4	1.75e-4
2020-01-01	6.00e8	11.0	0.85e-4	1.80e-4
2021-01-01	6.31e8	11.4	0.79e-4	1.90e-4

Figure 2: Tycho PC mode (grade 0-4) central CCD pointings from 2021 fit with the 2013-01-01 CALDB RMF (left) and the 2021-01-01 RMF, made available in this release, (right), showing improved residuals around the Si and S-Kα lines.

Comparison with Calibration Sources

A number of astrophysical sources are used to regularly monitor the state of the XRT calibration and check the level of agreement seen between other X-ray observatories, some results when testing the new RMFs follow.

Tycho – PC Mode

Figure 2 shows XRT PC mode (grade 0–4) Tycho SNR calibration observations from 2021-Sep and compares fits obtained with the previous CALDB 2013-01-01 RMF with the newly created 2021-01-01 RMF. The data are fit with a model derived from *XMM-Newton* MOS observations taken in 2000, and XRT observations taken in 2007 (when the effects of CTI and traps on XRT data were much reduced). The 2021-01-01 RMF response resolution matches the trap-corrected data far better, as illustrated by the reduced residuals around the Si and S-K lines, with a large improvement in the fit C-statistic of 2048. A residual gain offset of $-8.5\,\mathrm{eV}$ is seen across the $0.8 - 3.0\,\mathrm{keV}$ band, increasing to $41\,\mathrm{eV}$ at $5 - 8\,\mathrm{keV}$.

Cas A – WT Mode

Figure 3 shows XRT WT mode grade 0 observations of the Cas A SNR taken in 2021-Sep (red), compared to early post-launch 2005 data (black), fit with a model derived from *XMM-Newton* (pn and MOS1) and *NuSTAR* data. In the left panel the 2021 data (red) were fit with the 2013-12-12 RMF, while in the right panel the same data are fit with the newly released 2021-01-01 RMF, illustrating the improvement in the fit residuals around the S and Si-Kα lines, with a decrease in fit C-statistic of 8100. A residual gain offset of $-5.2\,\mathrm{eV}$ is seen across the $0.8 - 3.0\,\mathrm{keV}$ band, increasing to $-11\,\mathrm{eV}$ at $5 - 8\,\mathrm{keV}$.

SNR 1E0102.2–7219

Observations of the line-rich source SNR 1E0102.2–7219 were used to verify that the intrinsic resolution of the response kernel match the data at low energies for PC and WT mode.

Spectra from the autumn 2021 calibration observations are shown in figures 4 and 5 for PC mode (grade 0–4) and WT mode (grade 0), respectively, fit with the IACHEC reference model (v1.9 — see Plucinsky et al. 2012, SPIE, 8443, 12 and 2017 A&A 597 A35). The new RMFs show improvements to the fit C-statistic of 61 (PC) and 110 (WT) with small residual gain offsets of $-6\,\mathrm{eV}$ (PC) and $-8\,\mathrm{eV}$ (WT).
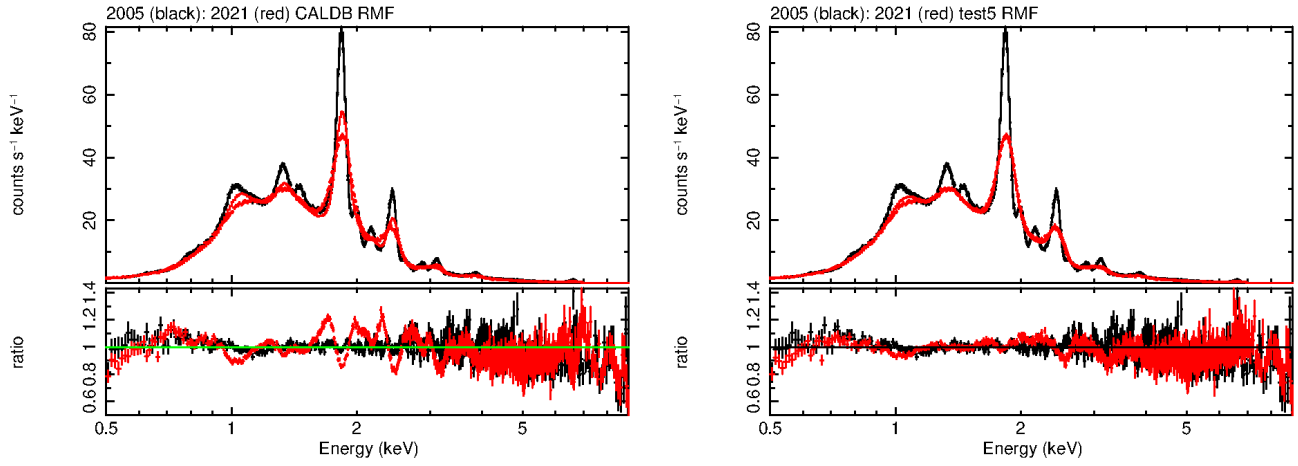
Figure 3: WT mode (grade 0) observation of the Cas A central CCD pointing from 2005 (black) and 2021 (red), in which the 2021 data are fit with the 2013-12-12 CALDB RMF (left) and the 2021-01-01 RMF made available in this release (right), with the latter showing improved residuals around the Si and S-Kα lines.
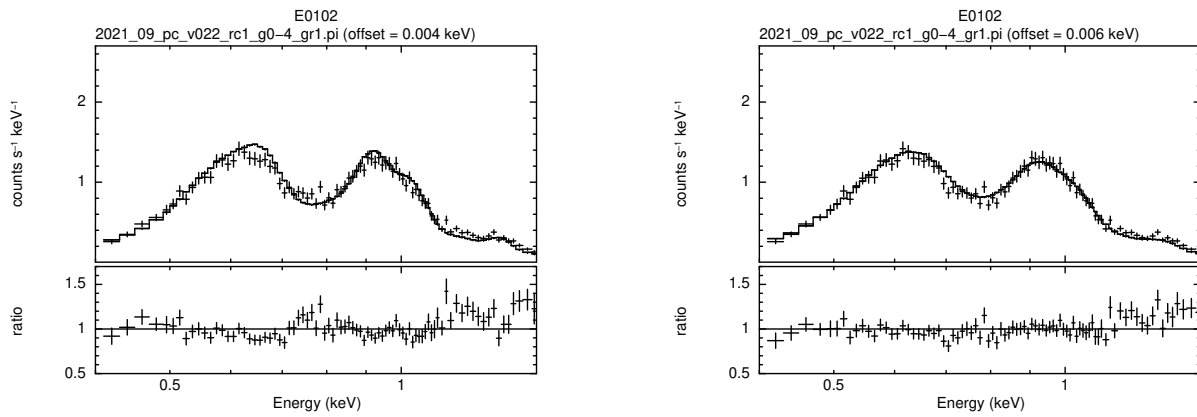

Figure 4: PC mode (grade 0–4) spectra of SNR 1E0102.2–7219 taken in 2021-Sep, fit with the 2013-01-01 CALDB RMF (left) and the 2021-01-01 RMF, made available in this release (right), with the latter showing an improvement in fit C-statistic of 61.
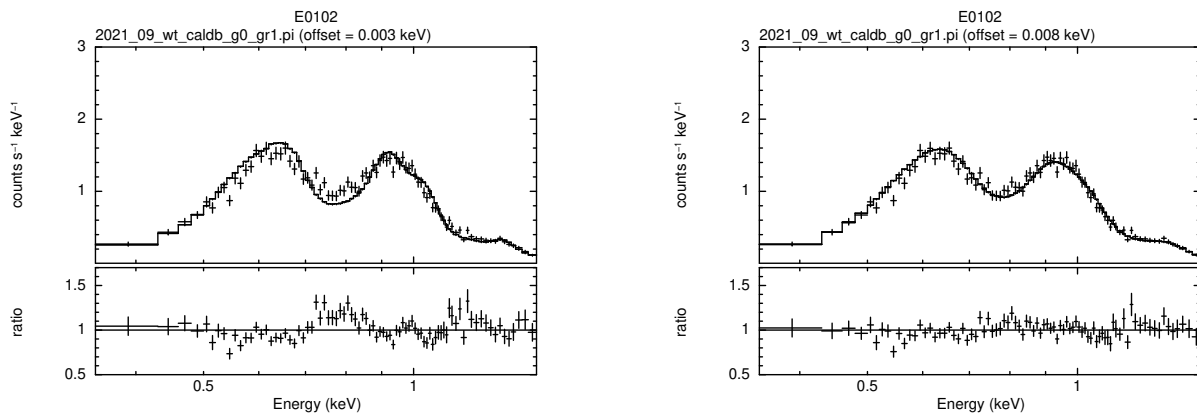

Figure 5: WT mode (grade 0) spectra of SNR 1E0102.2–7219 taken in 2021-Sep, fit with the 2013-12-12 CALDB RMF (left panel) and the 2021-01-01 RMF made available in this release (right), with the latter showing an improvement in fit C-statistic of 110.
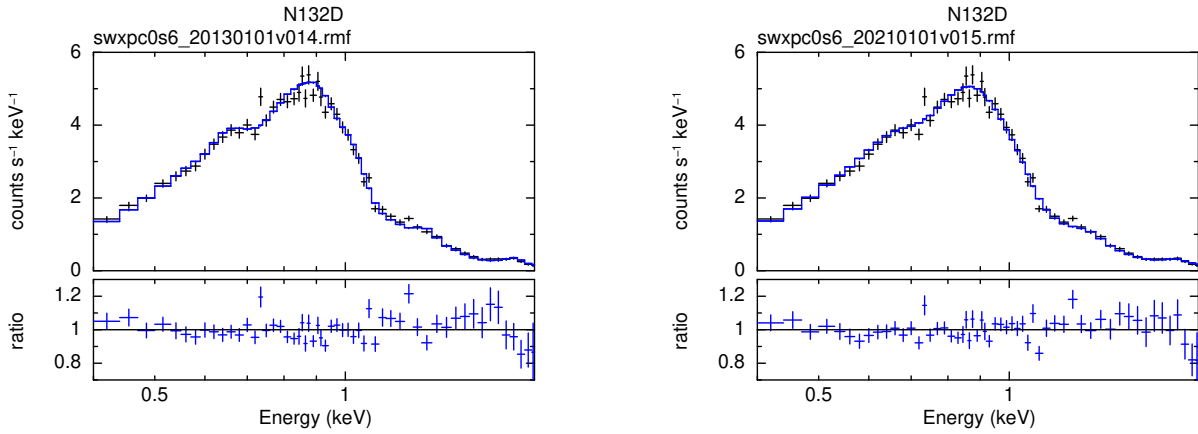
Figure 6: PC mode (grade 0) spectra of the SNR N132D taken in 2022-Mar, in which the data are fit with the 2013-01-01 CALDB RMF (left) and the 2021-01-01 RMF made available in this release (right), with the latter showing an improvement in fit C-statistic of 19.4.
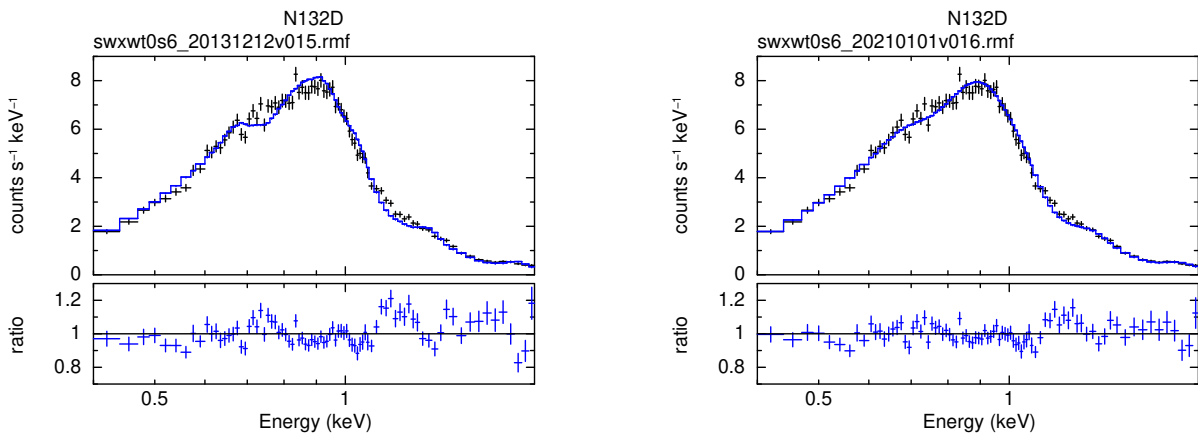

Figure 7: WT mode (grade 0) spectra of the SNR N132D taken in 2022-Mar, in which the data are fit with the 2013-12-12 CALDB RMF (left panel) and the 2021-01-01 RMF made available in this release (right), with the latter showing an improvement in fit C-statistic of 100.9.

N132D

The SNR N132D is observed in both PC and WT modes to test the accuracy of the gain / trap-mapping corrections below 1 keV. Spectra from the 2022 spring calibration observations are shown in figures 6 and 7 for PC mode (grade 0) and WT mode (grade 0–4), respectively, fit with the IACHEC model v2.10 (20170319). The new RMFs show improvements to the fit C-statistic of 19.4 (PC) and 100.9 (WT), with residual gain offsets of 1.2 eV (PC) and 25 eV (WT).

RX J1856.5–3754

The isolated neutron star RX J1856.5–3754 is considered to be a stable, soft X-ray source, modelled as a 62 eV blackbody (e.g. Beuermann et al., 2006, A&A, 458, 541). The source has been observed regularly since the substrate voltage changed in order to monitor the low energy response of the XRT. For both modes, the relative normalisation shows $\sim 10-25$ percent variations with time when fitting the data down to 0.3 keV (see SWIFT-XRT-CALDB-09_v19). We note that for soft sources such as this, small gain offsets of $10-20$ eV can be responsible for $10-15$ percent normalisation variations.

Figure 8 shows RX J1856.5–3754 grade 0 spectra taken in 2005 and 2021 for both PC and WT modes. The 2021 data are still well fit with a single temperature model down to 0.3 keV in both modes, with constant factors of 0.754 ± 0.025 (PC) and 0.880 ± 0.026 (WT) when compared to the IACHEC reference model (Burwitz 2017, priv.
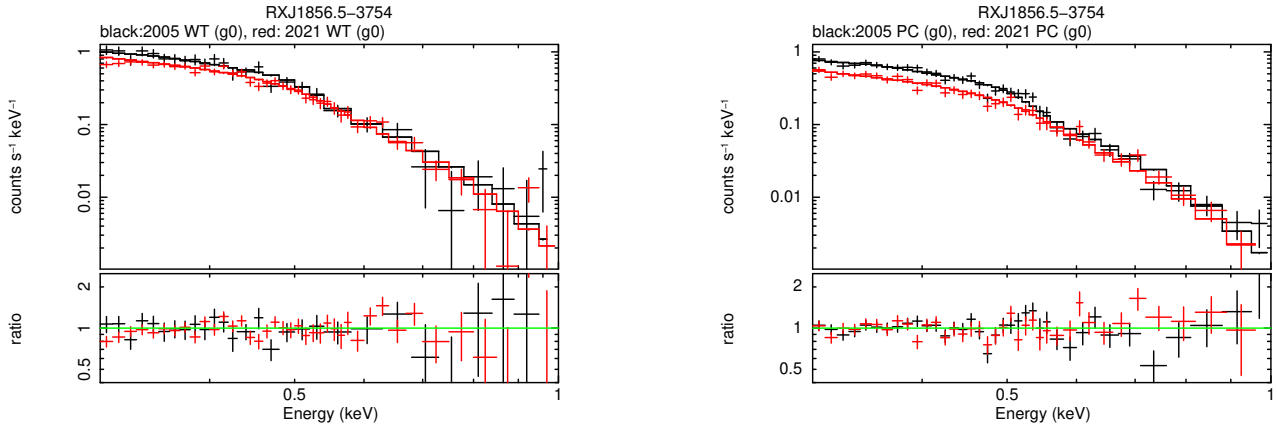
Figure 8: RX J1856.5–3754 WT (left) and PC (right) spectra (both grade 0) from 2005 (black) and 2021 (red), modelled with a 62 eV blackbody.

comm.).

Current limitations and future prospects

Experience has shown that the RMF/ARFs described here can be used reliably over the energy range $0.3 - 10\,\mathrm{keV}$ in PC mode and $0.3 - 10\,\mathrm{keV}$ in WT mode for data taken since 2021, and in general return fluxes which agree to within better than 15 per cent when compared with other X-ray missions.

The following considerations apply when using the RMFs/ARFs described here:

- The loss function, which is used by the simulator to describe how charge is incompletely collected from the X-ray interactions occurring near the surface of the device, shifts the redistribution peak of the lowest energy data down in energy. The loss function was derived from pre-launch laboratory calibration data obtained at the University of Leicester, using the central 200×200 pixel region of the detector, in order to be representative of XRT pointings taken close to the on-axis position. At the lowest input energies (C-Kα at $0.277\,\mathrm{keV}$; N-Kα at $0.392\,\mathrm{keV}$), the redistribution is seen to be non-uniform (see figure 9). If a source is positioned outside the central 200×200 region then it might show slightly worse redistribution than modelled by the RMF at the lowest energies (below $\sim 0.4\,\mathrm{keV}$).
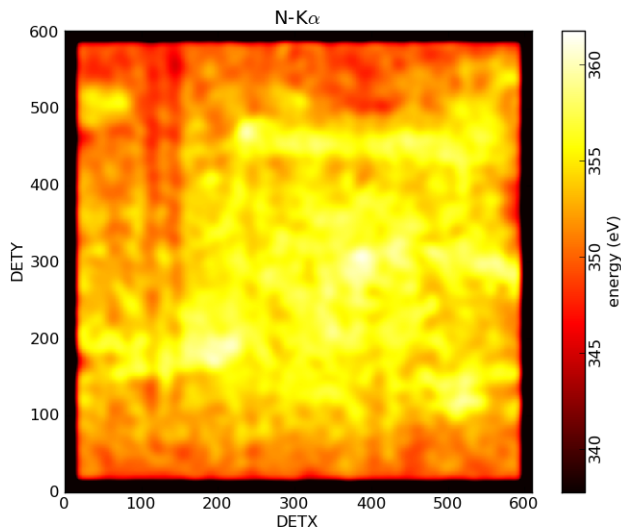
Figure 9: The spatial non-uniformity in the XRT spectral response over the surface of the detector at energies below $\sim 0.4\,\mathrm{keV}$ is illustrated in this image which shows the average event energy for N-Kα ($0.392\,\mathrm{keV}$) photons obtained from pre-launch laboratory calibration data. Event energy shifts of order $10 - 15\,\mathrm{eV}$ are visible outside the central 200×200 pixel region (from within which the response matrix loss function is calculated).

- High signal-to-noise WT spectra from sources with featureless continua (such as Mrk 421) typically show residuals of about 3 per cent, for example, near the Au-M_V edge (at 2.205 keV), the Si-K edge (at 1.839 keV), or the O-K edge (at 0.545 keV). Occasionally, however, residuals nearer the $10 - 15$ per cent level are seen, especially near the O-K edge, which are caused by small energy scale offsets (caused by inaccurate bias and/or gain corrections).

  Data taken in PC mode can be similarly effected, though observations taken in this mode tend to have fewer counts and hence a lower statistical quality, which make the residuals less apparent.

  Such residuals can often be improved through careful use of the *gain* command in XSPEC (by allowing the gain offset to vary by $\sim \pm 10 - 50$ eV).

- Also, observations of the soft NS RX J1856.5–3754 show that gain shifts of $10 - 20$ eV can cause $10 - 15$ per cent variations in the measured black-body normalisation.

- Note, while the epoch dependent files were generated with a certain range of dates in mind, our choice of date boundaries in making these RMFs reflects the continuous evolution of the CCD response, and does not relate to any quantised performance changes at these precise dates. Hence, if a source is observed either before (or after) a given RMF starting date epoch (from table P1 or table A1) then it is possible the RMFs from the following (or preceeding) epoch will work equally well.

- We attempt to keep a minimum usable energy of 0.3 keV for spectral fitting purposes. The values, obtained by averaging data over multiple snapshots, are somewhat approximate, as the minimum energy depends on the effective threshold, which in turn depends on trap depths and locations, and can vary with the position of the source on the detector. It is possible that a specific snapshot of data could have a minimum usable energy higher (or lower) than those suggested here, especially in WT mode (where the traps are deeper).

- WT observations of absorbed point sources show CCD detector position dependent redistribution effects which could cause residuals at low energies — see https://www.swift.ac.uk/analysis/xrt/rmfs.php. Updated WT mode position dependent RMFs for the 2021 epoch may be made availalbe at a later date. In the meantime, caution is advised when interpreting low energy residuals seen from observations of heavily absorbed sources in WT mode.

- We expect to provide additional epoch dependent RMFs for the period 2015 to 2020 in a forthcoming RMF release. However, given the large gap in time between the previous RMF release (2013) and this release (2021), it is possible that the 2021 RMFs will provide better fits to line or edge-like features for data taken prior to 2021. Hence, we suggest they are used to evaluate potential systematic effects when spectral fitting.

Summary of RMFs/ARFs currently in use

The following table summarises the RMFs and ARFs available and recommended for XRT spectral analysis and their time dependence.

Table A1: *Swift*-XRT RMFs/ARFs in use as of 2024-Apr-30.

Observation Date		Mode	Grade	File names
From	To			
2004-Dec-01	2006-Dec-31	WT	0-2	swxwt0to2s0_20010101v012.rmf swxs0_20010101v001.arf
			0	swxwt0s0_20010101v012.rmf swxs0_20010101v001.arf
		PC	0-12	swxpc0to12s0_20010101v012.rmf swxs0_20010101v001.arf
			0-4	swxpc0to4s0_20010101v012.rmf swxs0_20010101v001.arf
			0	swxpc0s0_20010101v012.rmf swxs0_20010101v001.arf
2007-Jan-01	2007-Aug-30	WT	0-2	swxwt0to2s0_20070101v012.rmf swxs0_20010101v001.arf
			0	swxwt0s0_20070101v012.rmf swxs0_20010101v001.arf
		PC	0-12	swxpc0to12s0_20070101v012.rmf swxs0_20010101v001.arf
			0-4	swxpc0to4s0_20070101v012.rmf swxs0_20010101v001.arf
			0	swxpc0s0_20070101v012.rmf swxs0_20010101v001.arf

Substrate voltage change from 0 V to 6 V on 2007-August-30

Observation Date		Mode	Grade	File names
From	To			
2007-Aug-31	2008-Dec-31	WT	0-2	swxwt0to2s6_20010101v015.rmf swxs6_20010101v001.arf
			0	swxwt0s6_20010101v015.rmf swxs6_20010101v001.arf
		PC	0-12	swxpc0to12s6_20010101v014.rmf swxs6_20010101v001.arf
			0-4	swxpc0to4s6_20010101v014.rmf swxs6_20010101v001.arf
			0	swxpc0s6_20010101v014.rmf swxs6_20010101v001.arf
2009-Jan-01	2010-Dec-31	WT	0-2	swxwt0to2s6_20090101v015.rmf swxs6_20010101v001.arf
			0	swxwt0s6_20090101v015.rmf swxs6_20010101v001.arf
		PC	0-12	swxpc0to12s6_20090101v014.rmf swxs6_20010101v001.arf
			0-4	swxpc0to4s6_20090101v014.rmf swxs6_20010101v001.arf
			0	swxpc0s6_20090101v014.rmf swxs6_20010101v001.arf

Table A1: continued.

2011-Jan-01	2012-Dec-31	WT	0-2	swxwt0to2s6_20110101v015.rmf swxs6_20010101v001.arf
			0	swxwt0s6_20110101v015.rmf swxs6_20010101v001.arf
		PC	0-12	swxpc0to12s6_20110101v014.rmf swxs6_20010101v001.arf
			0-4	swxpc0to4s6_20110101v014.rmf swxs6_20010101v001.arf
			0	swxpc0s6_20110101v014.rmf swxs6_20010101v001.arf
2013-Jan-01	2013-Dec-11	WT	0-2	swxwt0to2s6_20130101v015.rmf swxs6_20010101v001.arf
			0	swxwt0s6_20130101v015.rmf swxs6_20010101v001.arf
	TBC	PC	0-12	swxpc0to12s6_20130101v014.rmf swxs6_20010101v001.arf
			0-4	swxpc0to4s6_20130101v014.rmf swxs6_20010101v001.arf
			0	swxpc0s6_20130101v014.rmf swxs6_20010101v001.arf
2013-Dec-12	TBC	WT	0-2	swxwt0to2s6_20131212v015.rmf swxs6_20010101v001.arf
			0	swxwt0s6_20131212v015.rmf swxs6_20010101v001.arf
2021-Jan-01	—	WT	0-2	swxwt0to2s6_20210101v017.rmf swxs6_20010101v001.arf
			0	swxwt0s6_20210101v017.rmf swxs6_20010101v001.arf
		PC	0-12	swxpc0to12s6_20210101v016.rmf swxs6_20010101v001.arf
			0-4	swxpc0to4s6_20210101v016.rmf swxs6_20010101v001.arf
			0	swxpc0s6_20210101v016.rmf swxs6_20010101v001.arf

Note, the task XRTMKARF automatically reads in the correct ARF from the CALDB, based on information concerning the mode, grade and time of observation contained in the header of the input spectral file. The task also indicates to the screen which RMF is appropriate for the spectrum.

Useful Links

Summary of XRT RMF/ARF releases	http://www.swift.ac.uk/analysis/Gain_RMF_releases.html
XRT analysis threads at the UKSSDC, University of Leicester	http://www.swift.ac.uk/analysis/xrt/
XRT digest pages at the UKSSDC, University of Leicester	http://www.swift.ac.uk/analysis/xrt/digest.php
IACHEC website	http://web.mit.edu/iachec/